



NuFACT 2023

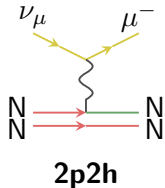
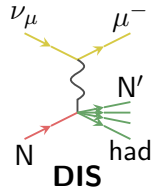
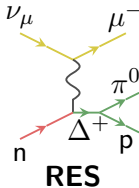
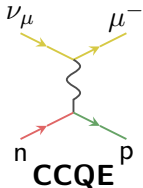
Impact of final-state de-excitation on modeling neutrino-nucleus interactions

Anna Ershova
anna.ershova@cea.fr

IRFU, CEA Saclay

August 25, 2023



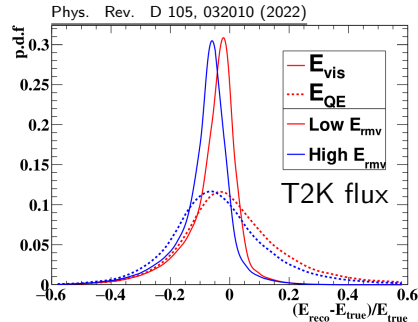


Energy reconstruction using only muon kinematics
(works well for **quasi-elastic reaction**):

$$E_\nu^{QE} = \frac{m_p^2 - (m_n - E_B)^2 - m_\mu^2 + 2(m_n - E_B)E_\mu}{2((m_n - E_B) - E_\mu + p_\mu \cos\theta_\mu)}$$

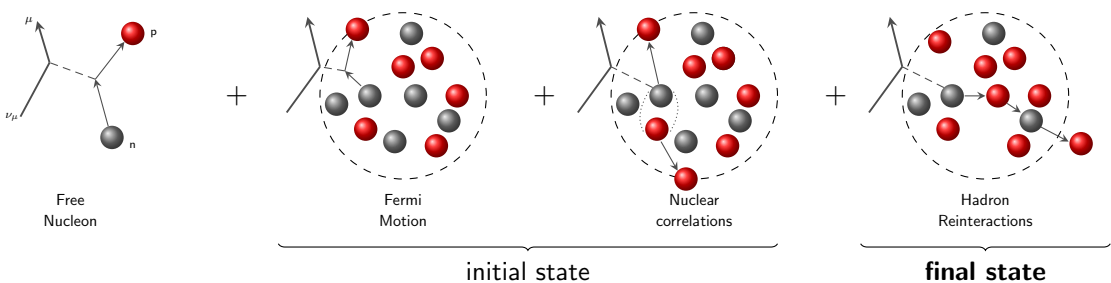
Energy reconstruction using **muon and kinetic energy of the nucleon**:

$$E_\nu^{vis} = E_\mu + T_N$$

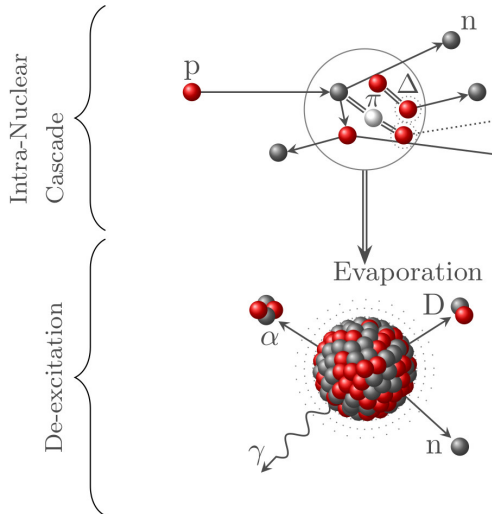


E_ν^{vis} , dashed line — QE formula
solid line — $\mu + N$ formula

$\mu + N$ formula gives us more **opportunities**, but also it creates more **challenges** for modelling and we need to **understand better nuclear effects** also on neutrons and protons.



We will focus on **CCQE** ν reaction channel and the **Final State Interactions (FSI)** that are described by **cascade models** and on the nuclear **excitation energy**.



Projectiles: baryons (nucleons, Λ , Σ), mesons (pions and Kaons) or light nuclei ($A \leq 18$). **No neutrinos** yet! We use neutrino vertex from  **NuWro** (widely used ν -nucleus MC generator).

Flexible tool: has been implemented in GEANT4 and GENIE

De-excitation: ABLA, SMM, GEMINI

We will use **ABLA**, since it proved to work for the **light nuclei** (Phys. J. Plus 130, 153 (2015))

First neutrino simulation results:
Phys. Rev. D 106, 3 (2022)



- Developed since 2005 in Wroclaw, Poland
- Optimized for use in **accelerator-based neutrino** oscillation experiments
- Multiple neutrino channels: QE, hyperon production, single pion production, 2p-2h, etc.

In this work, we use implemented **Spectral function** initial state model (but also checked RFG and reweighed INCL)

Cascade with space-like approach:

- The nucleus is a **continuous medium**
- mean free path: $\lambda_{free} = (\sigma \rho(r))^{-1}$
- probability to propagate **without** interaction: $P(\Delta x) = \exp(-\Delta x / \lambda)$
- **LFG** model is used during the **cascade**

Potential

Each nucleon in the nucleus has its **position and momentum** and moves **freely** in a square potential well. Nuclear model is essentially **classical**, with some additional ingredients to mimic quantum effects.

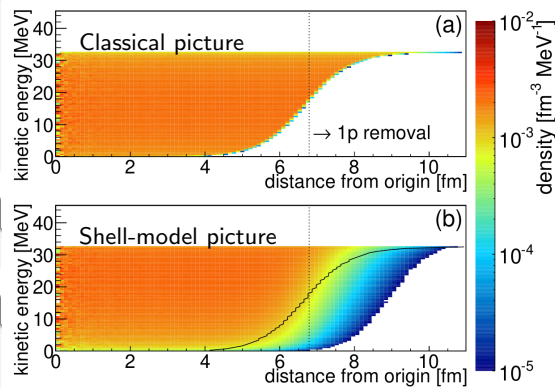
Pauli Blocking

criteria by which the state cannot be occupied

Events inside cascade

- decay/collision
- reflection/transmission with probability to **leave the nucleus as a nuclear cluster**

Space-kinetic-energy density of protons in ^{208}Pb



Phys. Rev. C 91, 034602 (2021)

Potential

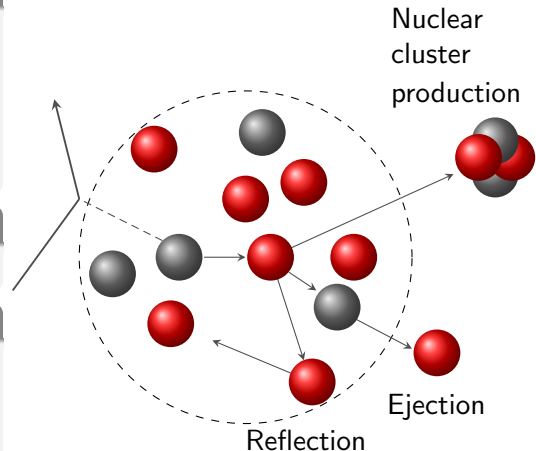
Each nucleon in the nucleus has its **position and momentum** and moves **freely** in a square potential well. Nuclear model is essentially **classical**, with some additional ingredients to mimic quantum effects.

Pauli Blocking

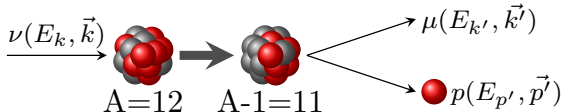
criteria by which the state cannot be occupied

Events inside cascade

- decay/collision
- reflection
- transmission with probability to **leave the nucleus as a nuclear cluster**



Excitation energy calculation



Experimental definition:

$$E_x^{\text{exp}} = E_{\text{missing}} - (M_A - M_{A-1} - M)$$

- A constant shift of missing energy by ~ 15.4 MeV leads to **non-physical, negative values**
- We use experimental data (J. Phys. G: Nucl. Part. Phys. 16 507 (1999)) to simulate discrete levels
- We assume all strength below the peak comes from the symmetric **$1p_{3/2}$ shell**

M_{A-1} is the rest mass of the $A - 1$ nucleus

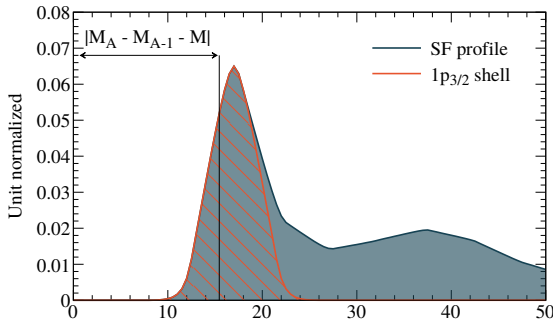
M_A is the rest mass of the initial A nucleus

M is the rest mass of the target nucleon

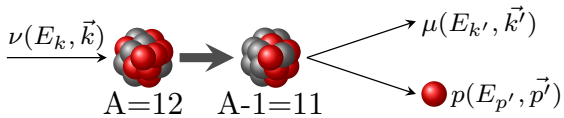
E_{missing} is the missing energy

For interaction on carbon,

$$M_A - M_{A-1} - M = 15.4 \text{ MeV}$$



Excitation energy calculation



For the continuous spectrum part, we can calculate excitation energy as:

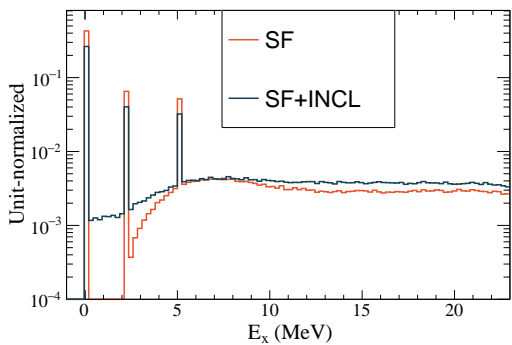
$$E_x = M_R^* - M_R, \text{ where:}$$

$$M_R^* = \sqrt{(E_k + M_A - E_{k'} - E_{p'})^2 - |\vec{p}_{\text{missing}}|^2}$$

Otherwise, we model **3 discrete peaks** with strength of 79%, 12%, and 9% (**p-shell**)

M_R^* is the mass of the excited remnant
 M_R is the rest mass of the remnant
 T_R is the kinetic energy of the excited remnant

p_{missing} is the missing momentum



Results

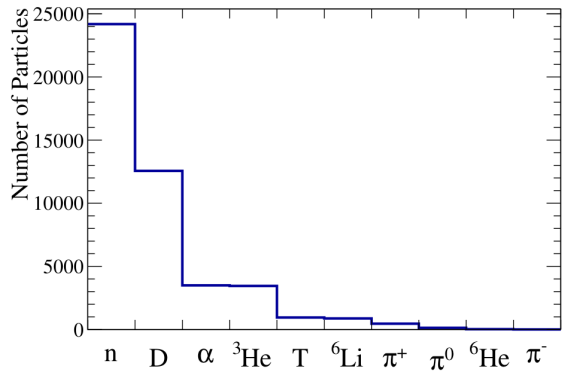
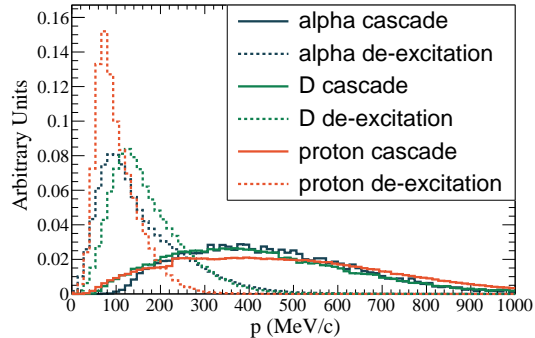
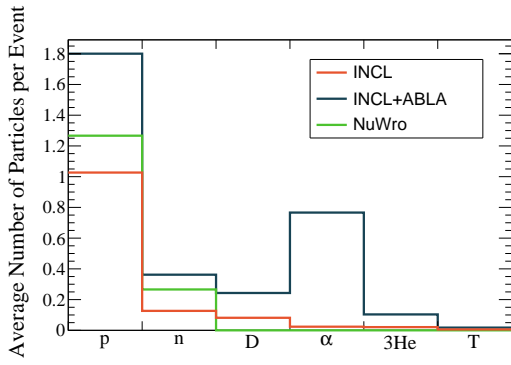


FIG. 11: Particles leaving the nucleus in events without proton in the final state in INCL.

In the last paper: Phys.Rev.D 106, 3 (2022)
we show the **nuclear cluster production for the first time** in FSI.

Now we study the impact of the subsequent **de-excitation modelling**, that predicts **more nuclear clusters**.

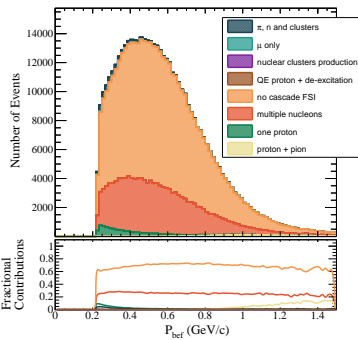
ABLA features a **massive production** of particles with **low momentum**.



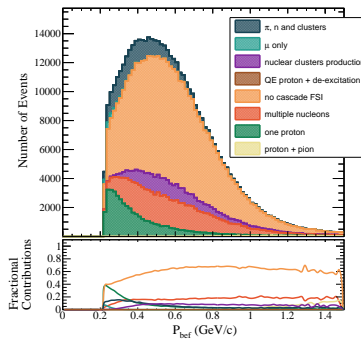
Momentum of nuclear clusters produced during the cascade and de-excitation

Proton momentum before FSI

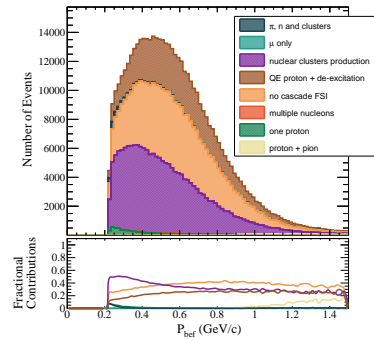
- Large fraction of "no FSI" events (i.e. proton untouched) is now **feature production of other particles** (and nuclear clusters) in the final state due to de-excitation
- Events with **only nucleon production** now feature **nuclear cluster production**



NuWro

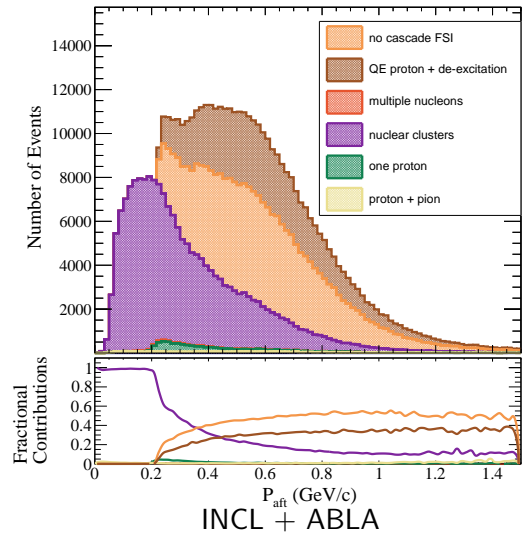
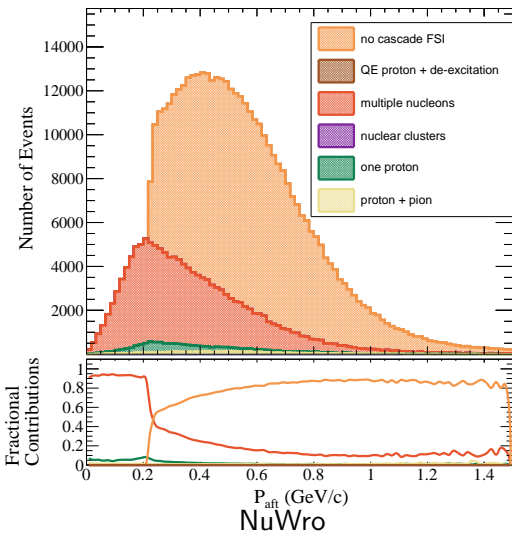


INCL



INCL + ABLA

INCL+ABLA simulation features **massive difference** in nucleon kinematics in comparison to NuWro

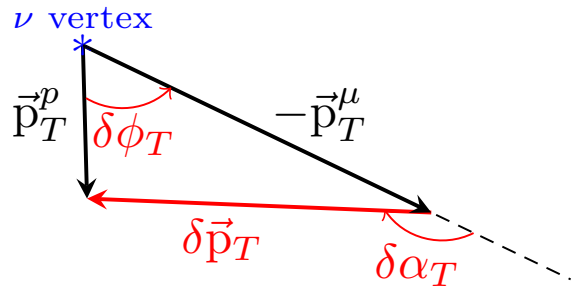


We use **Single Transverse Variables (STV)** that allow to disentangle different effects for better FSI estimation. STV are **observable** and **measurable**.

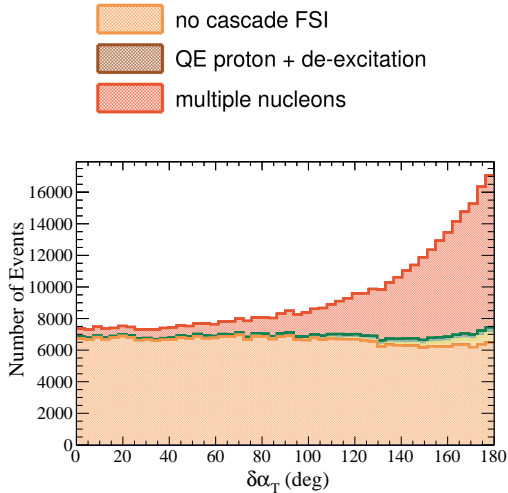
sensitive to FSI: $\delta\alpha_T = \arccos \frac{-\vec{k}'_T \cdot \delta\vec{p}'_T}{\vec{k}'_T \cdot \vec{p}'_T}$

sensitive to Fermi Motion:

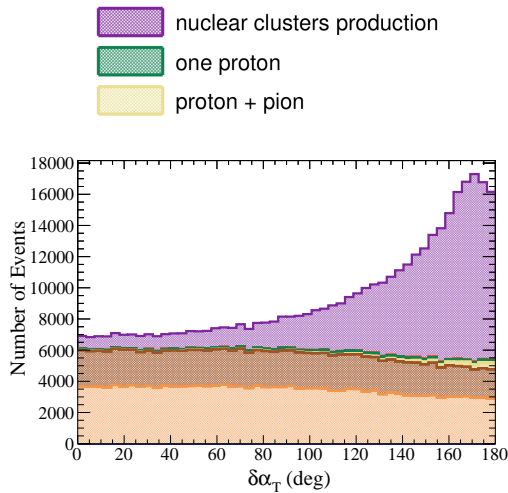
$$\delta\vec{p}_T = \vec{p}_T^{\bar{p}} + \vec{p}_T^{\bar{\mu}} = \vec{p}_T^{\bar{n}}$$



High $\delta\alpha_T$ strongly depends on FSI and is affected by de-excitation and Pauli blocking



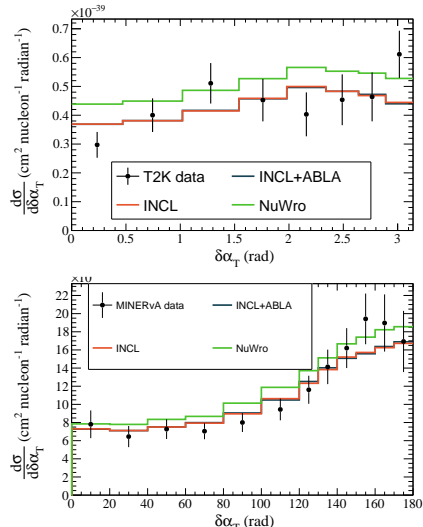
NuWro



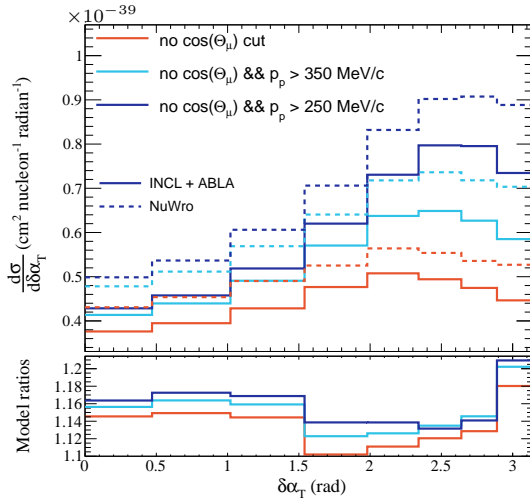
INCL+ABLA

Comparison to data

Current detector threshold in ND280 and MINERvA scintillators is **too large**, so we **cannot see the difference** between INCL and NuWro



Lower threshold provides better sensitivity to distinguish models



Using $\mu + p$ is **better** than using muon only, but here we show that we gain even **higher precision** by using all subleading particles

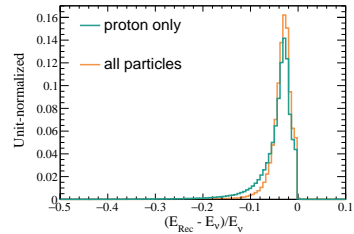
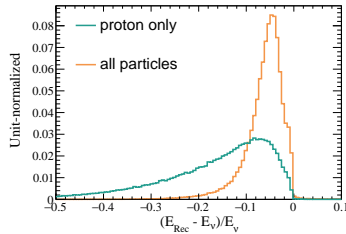
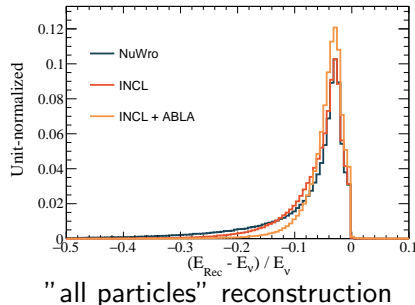
proton only:

$$E_{rec} = E_\mu + T_p$$



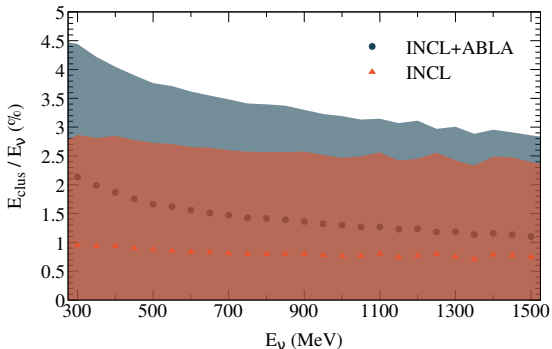
all particles (including clusters)

$$E_{rec} = E_\mu + \sum_i T_i$$

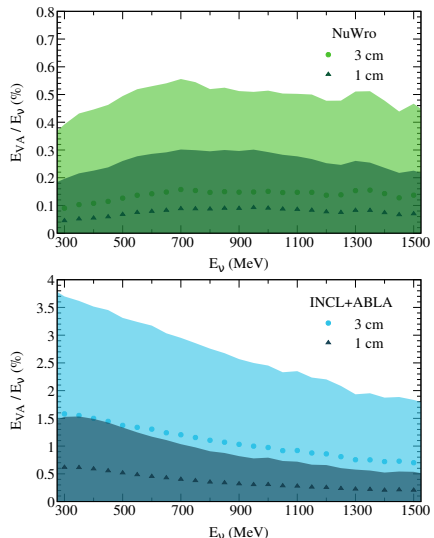


Vertex Activity as a fraction of neutrino energy

The **actual fraction** of neutrino energy going to the kinetic energy of the subleading hadrons is **non-negligible**.



What can be actually seen in the detector
(Birks quenching applied):



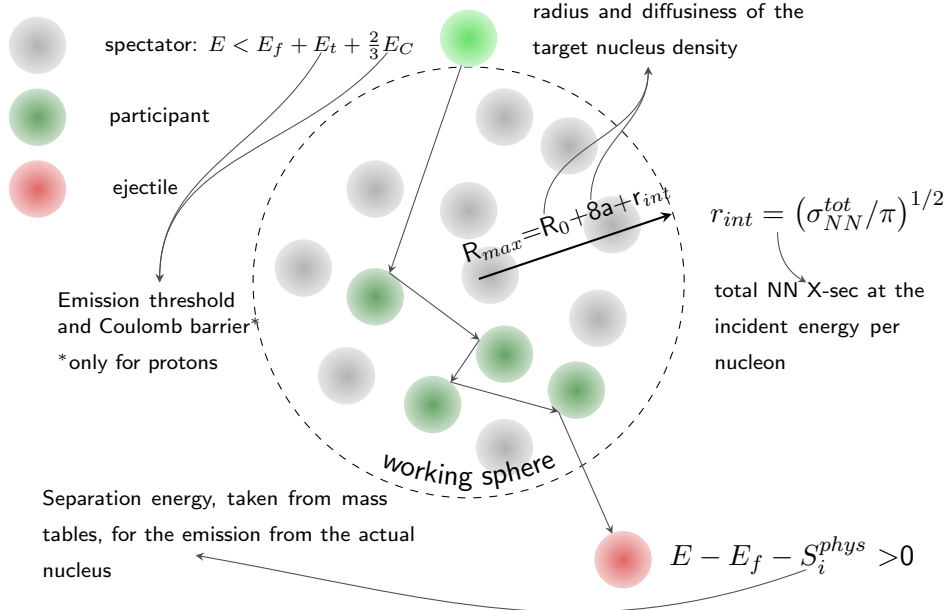
We compared the simulation of the final-state interactions between the **NuWro** and **INCL** cascade models in CCQE events. We coupled INCL cascade to the ABLA de-excitation model.

- "transparent events" are **no always** transparent: nuclear clusters may be produced
- INCL+ABLA simulation features **important difference** in nucleon kinematics in comparison to NuWro (and the other similar generator used in neutrino scattering)
- An essential novelty of this study is the **simulation of nuclear cluster production** during cascade and de-excitation. It is important for the understanding of the **vertex activity** and calorimetric method of ν **energy reconstruction**

For **precise neutrino energy reconstruction** (e.g. "calorimetric method") is important to include **vertex activity** ($\sim 1 - 2\%$), and to have proper model of it to correct for detector quenching. Large portion of VA comes from the **de-excitation**.

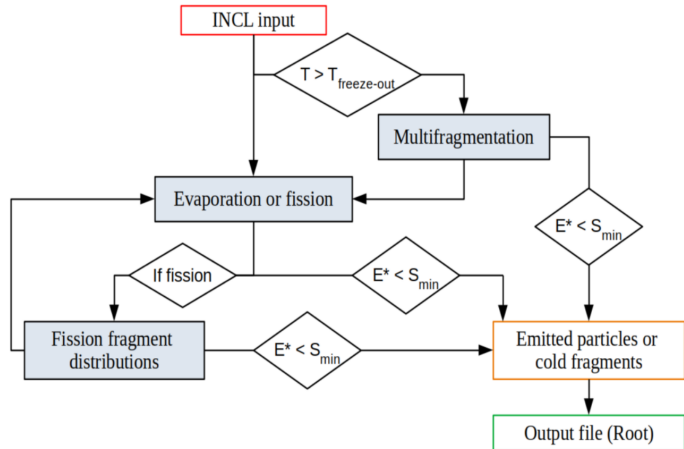
BACK UP

Standard INCL cascade



Phys. Rev. C 105, 014623 (2022)

The ablation model **ABLA** describes the **de-excitation** of an excited nuclear system through the emission of γ -rays, neutrons, light-charged particles, and intermediate-mass fragments (or fission in case of hot and heavy remnants).



$$T_{freeze-out} = \max \left[5.5, 9.33e^{(-2.82 \times 10^{-3} A_{rem})} \right]$$

S_{min} —minimum particle separation energy

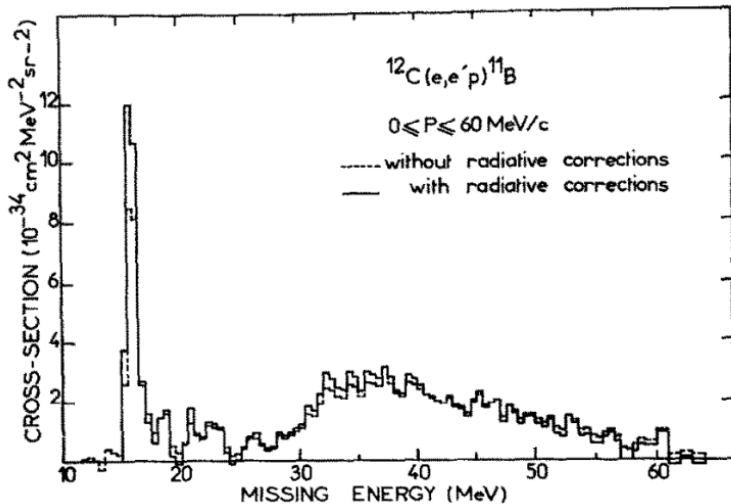


Fig. 7. Energy spectrum of the $^{12}\text{C}(\text{e}, \text{e}'\text{p})$ reaction before and after the radiative corrections.

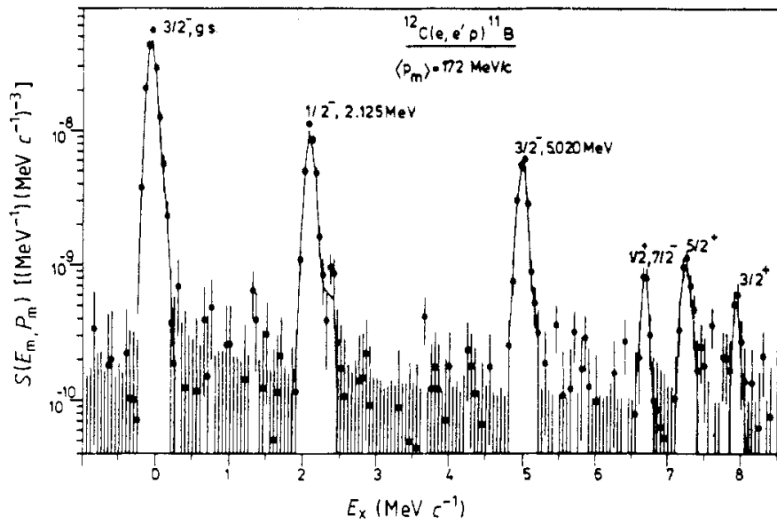


Figure 22. Excitation-energy spectrum of ^{11}B observed in the reaction $^{12}\text{C}(\text{e}, \text{e}'\text{p})$. Both negative and positive-parity final states are shown.